JOURNAL OF VACUUM SCIENCE AND TECHNOLOGY A

Etching properties of Pt thin films by inductively coupled plasma

Kwang-Ho Kwon, Chang-Il Kim, Sun Jin Yun, and Geun-Young Yeom

Citation: J. Vac. Sci. Technol. A **16**, 2772 (1998); doi: 10.1116/1.581420
View online: http://dx.doi.org/10.1116/1.581420
View Table of Contents: http://avspublications.org/resource/1/JVTAD6/v16/i5
Published by the AVS: Science & Technology of Materials, Interfaces, and Processing

Additional information on J. Vac. Sci. Technol. A

Journal Homepage: http://avspublications.org/jvsta
Journal Information: http://avspublications.org/jvsta/about/about_the_journal
Top downloads: http://avspublications.org/jvsta/top_20_most_downloaded
Information for Authors: http://avspublications.org/jvsta/authors/information_for_contributors

ADVERTISEMENT

Now Invent.™
The World's Manufacturer of Engineered & Advanced Materials
www.americanelements.com

Downloaded 29 May 2013 to 115.145.196.96. Redistribution subject to AVS license or copyright; see http://avspublications.org/jvsta/about/rights_and_permissions

Etching properties of Pt thin films by inductively coupled plasma

Kwang-Ho Kwon
Department of Electronic Engineering, Hanseo University, 360, Daegok-Ri, Haemi-Myun, Seosan-Si, Chung-Nam, 356-820, Korea

Chang-Il Kim[a)]
School of Electrical and Electronic Engineering, Chungang University, 221, Huksuk-Dong, Dongjak-Gu, Seoul, 156-756, Korea

Sun Jin Yun
Semiconductor Division, Electronics and Telecommunication Research Institute, Yusong P.O. Box 106, Taejon 305-600, Korea

Geun-Young Yeom
Department of Materials Engineering, Sungkyunkwan University, 300, Chunchun-Dong, Jangan-Gu, Suwon-Si, Kyunggi-Do, 440-300, Korea

(Received 9 October 1997; accepted 18 May 1998)

The inductively coupled plasma etching of platinum with Ar/Cl_2 gas chemistries is described. X-ray photoelectron spectroscopy (XPS) is used to investigate the chemical binding states of the etched surface with various $Ar/(Ar+Cl_2)$ mixing ratios. Atomic percentage of Cl element increases with increasing $Ar/(Ar+Cl_2)$ mixing ratio with the exception of $Ar/(Ar+Cl_2)$ mixing ratio of 1. At the same time, the peaks that seem to be subchlorinated Pt at XPS narrow scan spectra are found and Cl–Pt bonds rapidly increase at $Ar/(Ar+Cl_2)$ mixing ratio of 0.62. Quadrupole mass spectrometry (QMS) is used to examine the variations of plasma characteristics with various Ar/Cl_2 gas chemistries. QMS results show that Cl_2 molecules are converted to Cl radicals with adding Ar gas to Cl_2 plasma. QMS results support the increased atomic percentages of Cl elements on the etched Pt surface. Single Langmuir probe measures ion current density with various Ar/Cl_2 gas plasma. Ion current densities are used to investigate the ion bombardment effects on the etched surface. Thin film thickness measuring system, scanning electron microscope and a four-point probe are used to extract the Pt etching characteristics. The maximum etch rate of Pt is approximately 140 nm/min at the $Ar/(Ar+Cl_2)$ mixing ratio of 0.9. These results are consistent with XPS, QMS, and Langmuir probe data. © *1998 American Vacuum Society.* [S0734-2101(98)01505-X]

I. INTRODUCTION

Giga bit dynamic random access memory (DRAM) requires the capacitor of high dielectric films. Many researchers have been interested in the formation of high dielectric thin films. $Pb(Zr_{1-x}Ti_x)O_3$, $Ba_{1-x}Sr_xO_3$ and Sr_xTiO_3 have been promising candidates as high dielectric materials.[1–3] In order to preserve the high dielectric constant, the crystal structure of dielectric materials has to be a perovskite phase.[4] The formation of a perovskite phase depends on the crystal structure of substrate materials and requires nonoxidized surface of substrate materials. It is well known that the promising candidate to meet these requirements of substrate materials is Pt because of its chemical stability and good crystallinity. In DRAM processes, the fabrication of a capacitor consists of thin film deposition and dry etching. Although the technology to deposit the high dielectric films has been distinctly developed, very little work has been done in developing the etch technology for patterning the high dielectric films and Pt.[5,6] However, in order to form the high dielectric capacitor, the plasma etch technology of Pt has to be developed first.

Plasma process utilizing inductively coupled plasma (ICP) has emerged as a promising technique to meet the increasingly stringent requirements in microelectronics fabrication.[7,8] The high plasma density produced by ICP sources is particularly attractive for DRAM application. Some advantages in using this technique for etching is included higher etch rate and lower ion bombardment energies compared with conventional reactive ion etching.

In this study, the effects of additive Ar gas to Cl_2 plasma on the Pt etch characteristics were investigated. The dry etching technology using ICP sources was applied to etch Pt as a substrate material for the high dielectric capacitor. The chemical reaction on the etched surface, plasma characteristics, and Pt etch characteristics with Ar/Cl_2 gas chemistries were discussed.

Surface reaction of Pt etching was investigated with Ar/Cl_2 gas plasma using x-ray photoelectron spectroscopy (XPS) and quadrupole mass spectrometry. Ion current density was measured with Ar/Cl_2 gas plasma using single Langmuir probe. For the application to DRAM processes, Pt etching characteristics were also extracted using thin film thickness measuring system, and a four-point probe.

[a)]Author to whom correspondence should be addressed; electronic mail: cikim@cau.ac.kr

Downloaded 29 May 2013 to 115.145.196.96. Redistribution subject to AVS license or copyright; see http://avspublications.org/jvsta/about/rights_and_permissions

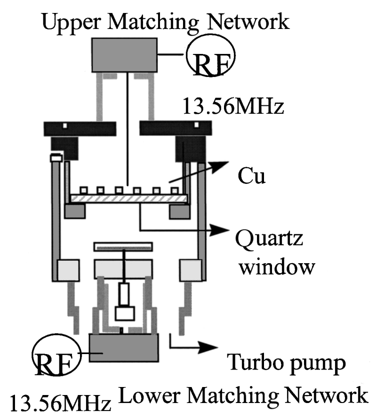

FIG. 1. Schematic diagram of experimental apparatus.

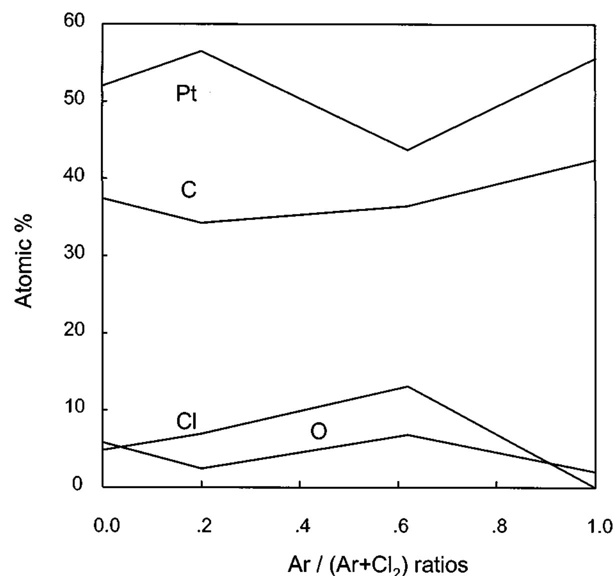

FIG. 2. XPS atomic counts of Pt surface with Ar/(Ar+Cl_2) gas mixing ratio.

II. EXPERIMENTAL DETAILS

The 5 in. Si substrates used for this study were doped with B (0.85-1.15 Ω cm), oriented (100), and chemically etched for 60 s using 1% HF:H_2O prior to chemical vapor deposition (CVD) growth. The substrates were coated with a 600 nm-thick layer of SiO_2 grown by low pressure CVD (SiH_4 $+O_2$, 420 °C, 240 mTorr). To enhance the adhesion of Pt on the oxide layer, a 75 nm-thick TiW (90%) was deposited prior to Pt deposition. Deposition of the Pt films was performed using a Varian 3180 dc sputtering system equipped with a 7 in. conical magnetron sputtering source. The Pt sputtering target was specified at 99.999% purity. Sputtering was performed in research-grade Ar at a pressure of 8 mTorr, and the distance from source to substrate was ~3.3 in. Typical sputtering power was 9.6 kW. These conditions resulted in a nominal deposition rate of ~1000 nm/min. During deposition, the substrate was grounded and the substrate temperature was held at 200 °C using a gas conduction heating. The final thickness of the sputtered Pt film was ~200–300 nm, and ~95% uniform across the surface of the 5 in. wafers. Film thickness was measured using a Tencor Model α-step 200 surface profiler.

Plasma etching of the Pt films was performed using a home-made ICP mode etching system. Figure 1 is a schematic diagram of experimental apparatus. A planar ICP etching equipment having a 3.5 turn spiral copper coil on the top of the chamber separated by a 1 cm-thick quartz window was used in this experiment. Note 13.56 MHz rf power was applied to the coil to induce inductively coupled plasma. Another 13.56 MHz rf power was applied to the substrate to induce bias voltage to the wafer. Wafers were placed on a bottom electrode. Substrate holder temperature during the Pt etch was held at ~50 °C using the circulation of cooling water. A Balzers turbo pump reduced residual gas pressure to below 5×10^{-5} Torr before the processing step. The Cl_2/Ar gas mixture was used for Pt etch and the total gas flow was 53 sccm. The Ar/(Ar+Cl_2) mixing ratio was changed from 0 to 1. ICP source power was constant at 600 W. Bias voltage was at −125 V and bias power was controlled to maintain the constant bias voltage. Etch rate was measured using a four-point probe and thin film thickness measuring system. To observe the etch profile, a ~300 nm thick plasma enhanced chemical vapor deposition film was deposited as a masking layer during Pt etching.

After removing the plasma etched samples from the etching system, the samples had been exposed to the atmospheric environment for approximately one day prior to XPS analysis. Compositional analysis of the Pt surface was performed using a VG Scientific ESCALAB 200R XPS with Mg $K\alpha$ (1253.6 eV) radiation operating at 250 W. A narrow scan spectra of all regions of interest was recorded with 20 eV pass energy in order to quantify the surface composition and identify the chemical binding state.

The plasma characteristic was extracted from QMS and single Langmuir probe. A quadrupole mass spectrometer (QMS; Balzers QMG/E 125) located at the sidewall of the process chamber was used to monitor species such as dissociated radicals in the plasma. The hole of 1 mm diam was formed to the wall of etching chamber and connected to the differential pumped system. The pressure of the port attached to QMS was maintained under 10^{-5} Torr. Single Langmuir probe was also inserted at the center of the chamber to measure the ion current density in the plasma. Ion current was saturated at approximately −20 V and was extracted at −40 V. Ion current density was calculated by dividing ion current into probe area.[9]

III. RESULTS AND DISCUSSION

A. Chemical binding states of etched surface

XPS analysis was carried out to investigate the etched Pt surface modification by using Ar/Cl_2 gas plasma. O, Pt, C, and Cl atoms were detected on the etched surface. However, Ar did not exist on the etched surface. O and C were observed and were caused by air exposure of the etched samples prior to XPS analysis.

Downloaded 29 May 2013 to 115.145.196.96. Redistribution subject to AVS license or copyright; see http://avspublications.org/jvsta/about/rights_and_permissions

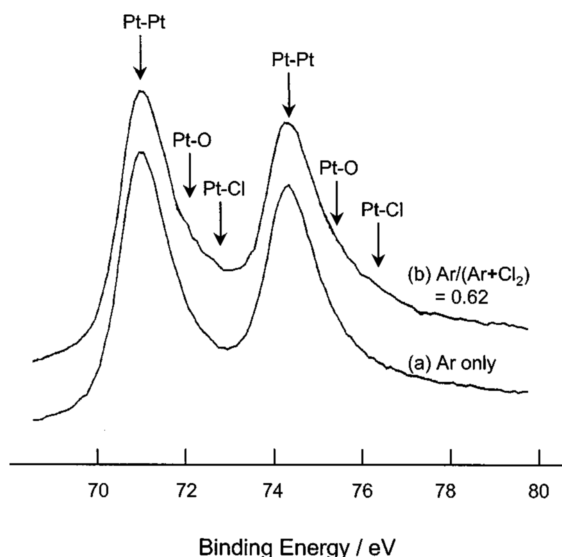

FIG. 3. Pt $4f$ narrow scan spectra at $Ar/(Ar+Cl_2)$ ratios of (a) 1 and (b) 0.62.

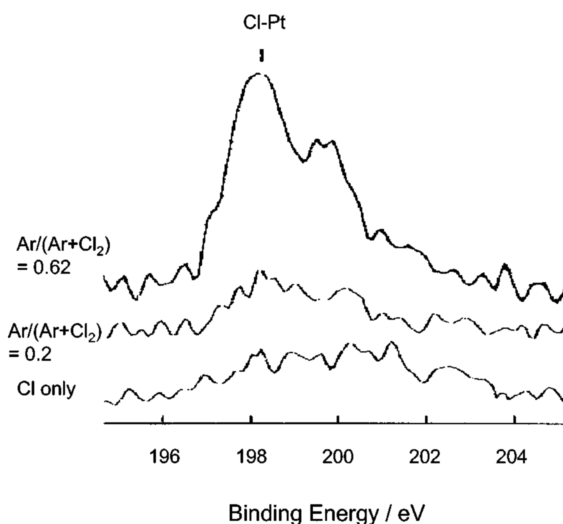

FIG. 4. Cl $2p$ narrow scan spectra at various $Ar/(Ar+Cl_2)$ mixing ratio.

Figure 2 represents the XPS atomic counts of the Pt surface with Ar/Cl_2 gas mixing ratio. In Fig. 2, the atomic percentage of chlorine has the maximum value at $Ar/(Ar+Cl_2)$ of 0.62. Under $Ar/(Ar+Cl_2)$ ratio of 0.62, chlorine increased with increasing Ar flow rate in spite of decreasing Cl_2 partial pressure in the plasma. At the same time, the atomic percentage of Pt has the minimum value at $Ar/(Ar+Cl_2)$ ratio of 0.62. This means that the residual layer formed on the etched surface at 0.62 of $Ar/(Ar+Cl_2)$ is thicker than those at other etching conditions.

XPS narrow scan analysis was carried out to examine the chemical binding states of each element on the Pt surface with $Ar/(Ar+Cl_2)$ ratio. Figure 2 shows Pt narrow scan spectra. Figures 3(a) and 3(b) represent the Pt $4f$ spectra with $Ar/(Ar+Cl_2)$ ratios of 1 and 0.62, respectively. Figure 3(a) shows that the Pt $4f$ spectrum can be resolved into two chemical components as Pt–Pt and Pt–O. The peaks at 71 and 74.4 eV binding energies correspond to Pt $4f_{7/2}$ and Pt $4f_{5/2}$ of elemental Pt, respectively. At the same time, Pt $4f_{7/2}$ due to suboxided Pt is also found at the binding energy of 72 and 75.5 eV because 74 and 75 eV binding energies are observed for normal Pt–O bonds in PtO and PtO_2,[10] respectively. This implies that Pt atoms on the surface mainly exist as the chemical state of elemental Pt. It is also found in this figure that the peak intensities of Pt–O bonds are small. This seems to result from the chemical stability of Pt. Meanwhile, the Pt $4f$ narrow spectra was obtained at the $Ar/(Ar+Cl_2)$ mixing ratios of 0, 0.2, and 1 were nearly same. This implies that Cl atoms exist insignificantly on the etched surface in these gas mixing conditions. However, it is found that Fig. 3(b) is changed. In comparison to Fig. 3(a), it is found that the peak intensities corresponding to the binding energies of 72.8 and 76.3 eV were increased. These peak increases seem to result from the bond with a high electronegative element such as chlorine. This can be inferred since Cl atomic percentage rapidly increases but O is insignificantly changed in Fig. 2. At the same time, Pt–Cl bond is detected at the higher binding energy compared to Pt–O bond because Cl atom is more electronegative than O atom. Meanwhile, these peaks result from subchlorinated Pt because 73.5 and 75.3 eV binding energies are observed for normal Pt–Cl binding states of $PtCl_2$ and $PtCl_4$, respectively.

Figure 4 represents Cl $2p$ narrow scan spectra with various $Ar/(Ar+Cl_2)$ mixing ratios. Cl $2p$ spectrum is entirely composed of single component as Cl–Pt. Cl–Pt bond is observed at 198 eV and formed as a doublet. At $Ar/(Ar+Cl_2)$ ratio of 0.62, Cl–Pt bond increases significantly and this result agrees with Fig. 2. This means that the majority of Cl atoms combine with Pt. Meanwhile, Cl–O bond was not detected.

B. Plasma characteristics

In order to examine the cause of Fig. 2, the plasma species densities were obtained by QMS. Table I shows the relative density of plasma species with various $Ar/(Ar+Cl_2)$ gas mixing ratio. In this table, Ar species increase with increasing $Ar/(Ar+Cl_2)$ ratio. This seems to be due to the increase of Ar partial pressure in the plasma. At the same time, Cl_2 species density decreases rapidly at $Ar/(Ar+Cl_2)$ mixing ratio of 0.9. However, Cl radical density insignificantly decreases between 0 and 0.9. These indicate that the dissociation of Cl_2 molecules was enhanced by additive Ar and Cl_2 molecules were converted into Cl radicals. This

TABLE I. Relative plasma species density with various $Ar/(Ar+Cl_2)$ mixing ratio.

$Ar/(Ar+Cl_2)$	Cl radicals	Cl_2 molecules	(Arb. unit) Ar species
0.0	3.8	3.4	0.0
0.1	4.0	3.6	1.2
0.9	3.4	0.5	9.0
1.0	0.0	0.0	9.5

Downloaded 29 May 2013 to 115.145.196.96. Redistribution subject to AVS license or copyright; see http://avspublications.org/jvsta/about/rights_and_permissions

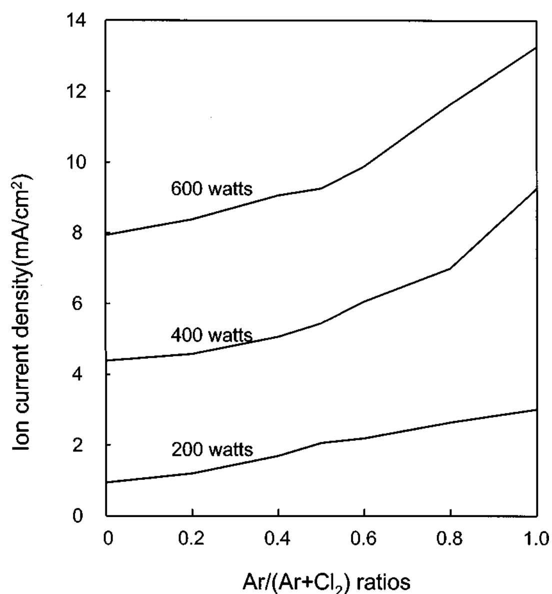

FIG. 5. Ion current density as a function of various Ar/(Ar+Cl_2) gas mixing ratio and ICP source power.

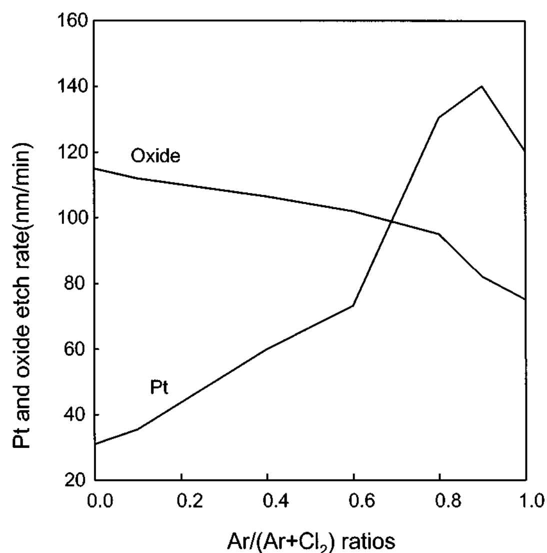

FIG. 6. Pt and oxide etch rates as a function of Ar/(Ar+Cl_2) mixing ratio.

means that the additive Ar has an effective role of the Cl_2 dissociation and an important effect on Pt reaction with Cl elements.

Figure 5 represents the ion current density with various gas mixing ratio and ICP source power by single Langmuir probe. This figure shows that ion current density increase with increasing Ar/(Ar+Cl_2) ratio. This result can be explained by the fact that Ar makes a role of neutral scatterer.[11] This implies that ion bombardment effects on the etched surface are enhanced with increasing Ar/(Ar+Cl_2) ratio. The enhanced ion bombardment effects increase the reaction of Cl species with Pt. Therefore, in Fig. 2, it is confirmed that Cl atomic percentage at Ar/(Ar+Cl_2) ratio of 0.62 is higher than that at other Ar/(Ar+Cl_2) ratios because ion bombardment effects and Cl radical density are increased with increasing Ar/(Ar+Cl_2) ratio. At the same time, it is also found that ion current density increases with increasing source power. This seems to be caused by the increased electron density. Thus, the increased electron density enhances the collision with neutral species and increases the ionization of neutral species.

C. Pt etch characteristics

Figure 6 represents Pt and oxide etch rates as a function of Ar/(Ar+Cl_2) mixing ratio. This figure shows that Pt etch rate increases with increasing gas ratio, but it decreases at Ar/(Ar+Cl_2) mixing ratio of 1. At the same time, oxide etch rate decreases with increasing Ar/(Ar+Cl_2) mixing ratio. It is also found that Pt etch rate at Ar/(Ar+Cl_2) of 0.9 is higher than that at Ar/(Ar+Cl_2) of 1. Pt etching would progress by physical sputtering effects at Ar/(Ar+Cl_2) ratio of 1. Therefore it is confirmed that increased etch rate at Ar/(Ar+Cl_2) of 0.9 results from the enhanced chemical reaction between Pt and Cl radicals and the increased ion bombardment effects as mentioned. Meanwhile, the decrease of oxide etch rate seems to be resulted from the decrease of Cl_2 partial pressure.

IV. CONCLUSION

The chemical binding states of etched surface with various Ar/(Ar+Cl_2) mixing ratios were investigated by using XPS. The peaks were found due to subchlorinated Pt in the XPS narrow scan spectra and Cl–Pt binding states rapidly increased with increasing Ar/(Ar+Cl_2) mixing ratio. QMS results showed that Cl_2 molecules were converted to Cl radicals with additive Ar gas in the Cl_2 plasma. These results support the cause that the atomic percentages of Cl elements increase with increasing Ar/(Ar+Cl_2) mixing ratio on the etched Pt surface. Single Langmuir probe results showed that the ion bombardment effects on the etched surface increased with increasing Ar/(Ar+Cl_2) mixing ratio. Meanwhile, the maximum etch rate of Pt was 140 nm/min at the Ar/(Ar+Cl_2) mixing ratio of 0.9.

In this study, it was confirmed that the increase of Pt etch rate resulted from increasing the ion bombardment effects and the reactive Cl radicals with additive Ar gas to Cl_2 plasma.

ACKNOWLEDGMENTS

The authors would like to acknowledge the support of the Korea Science and Engineering Foundation for this study through Contact No. 961-0918-093-2.

Presented at the 44th National Symposium of the American Vacuum Society, San Jose, CA, 20–24 October 1997.

[1]H. Tomonari, T. Ishiu, K. Sakata, and T. Takenaka, Jpn. J. Appl. Phys., Part 1 **31**, 2998 (1992).
[2]K. Koyama, T. Sakuma, S. Yamamichi, H. Aoki, S. Ohya, Y. Miyasaka, and T. Kikkawa, Tech. Dig. Int. Electron Devices Meet. 823 (1991).
[3]T. Sahuma, S. Yamamichi, S. Matsubara, H. Yamaguchi, and Y. Mi-

Downloaded 29 May 2013 to 115.145.196.96. Redistribution subject to AVS license or copyright; see http://avspublications.org/jvsta/about/rights_and_permissions

yasaka, Appl. Phys. Lett. **57**, 2431 (1990).
[4]H. Maiwa, N. Ichinose, and K. Okazaki, Jpn. J. Appl. Phys., Part 1 **31**, 3029 (1992).
[5]S. Yokoyama, Y. Ito, K. Ishihara, K. Hamada, S. Onish, J. Kudo, and K. Sakiyama, Jpn. J. Appl. Phys., Part 1 **34**, 767 (1995).
[6]S. Onish, K. Hamada, K. Ishhara, Y. Ito, S. Yokoyama, J. Kudo, and K. Sakiyama, Tech. Dig. Int. Electron Devices Meet. 843 (1994).
[7]J. Amorim, H. S. Maciel, and J. P. Sudano, J. Vac. Sci. Technol. B **9**, 362 (1991).
[8]J. Hopewood, C. R. Guarnieri, S. J. Whitehair, and J. J. Cuomo, J. Vac. Sci. Technol. A **11**, 152 (1993).
[9]R. Patrick, P. Schoenborn, H. Toda, and F. Bose, J. Vac. Sci. Technol. A **11**, 1296 (1993).
[10]*The Handbook of Electron Spectroscopy for Chemical Analysis* (Perkin Elmer, Eden Prairie, MN, 1978), p. 152.
[11]C. B. Zarowin, J. Electrochem. Soc. **130**, 1144 (1983).

Downloaded 29 May 2013 to 115.145.196.96. Redistribution subject to AVS license or copyright; see http://avspublications.org/jvsta/about/rights_and_permissions